

# Mesoscopic p-wave superconductor near the phase transition temperature

Bor-Luen Huang and S.-K. Yip  
*Institute of Physics, Academia Sinica, Taipei, Taiwan*  
 (Dated: December 14, 2012)

We study the finite-size and boundary effects on a p-wave superconductor in a mesoscopic rectangular sample using Ginzburg-Landau (GL) and quasi-classical (QC) Green's function theory. Except for a square sample with parameters far away from the isotropic weak-coupling limit, the ground state near the critical temperature always prefers a time-reversal symmetric state, where the order parameter can be represented by a real vector. For large aspect ratio, this vector is parallel to the long side of the rectangle. Within a critical aspect ratio, it has instead a vortex-like structure, vanishing at the sample center.

PACS numbers: 74.78.Na, 74.20.De, 74.20.Rp

Studies of multicomponent superfluids and superconductors have excited many for decades because of the diversity of textures, complex vortex structures and collective modes. The superfluid  $^3\text{He}$  with spin-triplet order parameter [1, 2] is a well-established example. Many studies also show that superconductors with multicomponent order parameters can also be found in, for example,  $\text{UPt}_3$  [3, 4] and  $\text{Sr}_2\text{RuO}_4$  [5, 6]. Recently, studies of multicomponent superconductor in a confined geometry draw much attention due to advancements in nanofabrication. Experiments claimed to find half-quantum vortices [7] and the Little-Parks effect [8] in  $\text{Sr}_2\text{RuO}_4$  quantum ring. Surfaces are expected to have non-trivial effects on such superconductors. Some theoretical works show that surface currents are present in broken time-reversal symmetric superconductors.[9–11] In considering Ru inclusions, Sigrist and his collaborators [12] have shown that a time-reversal symmetry state can be favored near the interface between Ru and  $\text{Sr}_2\text{RuO}_4$  due to the boundary conditions. In our previous work [13], considering a thin circular disk with smooth boundaries and applying Ginzburg-Landau (GL) theory, we have shown that a two-component p-wave superconductor can exhibit multiple phase transitions in a confined geometry. At zero magnetic field, the superconducting transition from the normal state was found to be always first to a time-reversal symmetric state (with one exception which we discussed in more detail below), even though the bulk free energy may favor a broken time-reversal symmetry state, which can exist at a lower temperature. This time-reversal symmetric state has a vortex-like structure, with order parameter vanishing at the center of the disk. We have also argued there that these features are general, do not rely on the GL approximation and should exist for also general geometries. [14]

In this paper, we shall show that this is indeed true by considering rectangular and square samples. For rectangular samples with large aspect ratios, we show that the phase transitions are first to a state with order parameter being a real vector parallel to the long side of the sample. For smaller aspect ratios, the state near the transition temperature is again a time-reversal symmetric state with a vortex at the center, much like what we

found for the circular disk (again with an exception to be mentioned below). We show these results using both GL and quasiclassical (QC) theories. The results from these two approaches are qualitatively similar except for the critical sizes and aspect ratios obtained.

We shall thus consider a superconductor where its orbital part is given by  $\vec{\eta} = \eta_x \hat{x} + \eta_y \hat{y}$ . We shall consider the dependences of  $\eta_x$  and  $\eta_y$  on the coordinates  $x, y$ , assuming that they are constant along the  $z$  direction. We assume the length of the sample in  $x$  direction is  $L$  and the width in  $y$  direction is  $W$ , and these surfaces are smooth. The effects of rough boundary have been discussed in Ref.[13] for the circular disk. We shall also limit ourselves to zero external magnetic fields. Near the transition temperature, the magnetic field generated by the supercurrent is also negligible, hence the vector potential can always be ignored.

First, we study this system via GL theory. The GL free energy density per unit area for the bulk,  $\mathcal{F}_b$ , can be written as

$$\mathcal{F}_b = \alpha(\vec{\eta}^* \cdot \vec{\eta}) + \dots \quad (1)$$

where  $\alpha = \alpha'(t - 1)$  with  $\alpha' > 0$ ,  $t \equiv T/T_c^0$  is the ratio of the temperature  $T$  relative to the bulk transition temperature  $T_c^0$ , and  $\dots$  represents terms higher power in the order parameter which are irrelevant below since we are interested only in the physics at the (modified) transition temperature  $T_c$ . In the presence of spatial variations, there is an additional contribution to the free energy given by

$$\mathcal{F}_g = K_1(\partial_j \eta_l)(\partial_j \eta_l)^* + K_2(\partial_j \eta_j)(\partial_l \eta_l)^* + K_3(\partial_j \eta_l)(\partial_l \eta_j)^* + K_4[(\partial_x \eta_x)^2 + (\partial_y \eta_y)^2], \quad (2)$$

where repeated indices  $j, l$  in the first three terms are summed over  $x, y$ , and the last term describes crystal anisotropy.[15] Within weak coupling approximation, particle-hole symmetry, and for an isotropic Fermi surface,  $K_1 = K_2 = K_3 > 0$  and  $K_4 = 0$ , but we shall treat these coefficients as general parameters.

The GL equations need to be accompanied by boundary conditions. The perpendicular component of the order parameter at the surface should vanish [17]. Thus,

for a point at the surface where the normal is  $\hat{n}$ ,  $\hat{n} \cdot \vec{\eta} = 0$ . For a smooth surface, the parallel component  $\eta_{\parallel}$  should have vanishing normal gradient [17]. That is, at the surface,  $(\hat{n} \cdot \nabla)\eta_{\parallel} = 0$ .

GL equations for  $\eta_{x,y}$  can be obtained by the variation principle. Near the critical temperature, we can linearize these equations. The easiest way to match the boundary conditions is to superimpose the Fourier components. Written in matrix form, the GL equations for the Fourier component  $\vec{q}$  become

$$\begin{pmatrix} K_1 q^2 + K_{234} q_x^2 & K_{23} q_x q_y \\ K_{23} q_x q_y & K_1 q^2 + K_{234} q_y^2 \end{pmatrix} \begin{pmatrix} \eta_{x,\vec{q}} \\ \eta_{y,\vec{q}} \end{pmatrix} = \alpha'(1-t) \begin{pmatrix} \eta_{x,\vec{q}} \\ \eta_{y,\vec{q}} \end{pmatrix}. \quad (3)$$

Here,  $\vec{q}$  is the wavevector,  $q^2 = q_x^2 + q_y^2$ ,  $K_{23} = K_2 + K_3$ , and  $K_{234} = K_2 + K_3 + K_4$ .

It is easy to find that, if  $q_x = 0$  or  $q_y = 0$ , Eq.(3) decouples. We obtain either (i)  $\eta_{x,\vec{q}} \neq 0$  with  $\eta_{y,\vec{q}} = 0$  or (ii)  $\eta_{y,\vec{q}} \neq 0$  with  $\eta_{x,\vec{q}} = 0$ . We call these solutions as A phases. In case (i), we have two possibilities. One is  $\hat{q} = \hat{x}$  and the critical temperature is determined by  $\alpha'(1-t) = K_{1234} q^2$ . Because  $\eta_x(x)$  is independent of  $y$ , the possible solutions are  $\eta_x = X \sin \frac{m\pi x}{L}$ , satisfying the boundary conditions,  $\eta_x = 0$ , at  $x = 0$  and  $L$ . Here  $X$  is a constant and  $m$  is an integer. The best choice is  $m = 1$  and the critical temperature is  $\alpha'(1-t) = K_{1234}(\pi/L)^2$ . We call this the  $A_1$  phase. The other is  $\hat{q} = \hat{y}$ . The order parameter  $\eta_x(y)$  is independent of  $x$ . Thus it is not possible to satisfy the boundary conditions at  $x = 0$  and  $L$ . In case (ii), the best solution is  $\eta_y \propto \sin \frac{\pi y}{W}$ , which is just the solution in case (i) with  $x \leftrightarrow y$ . The critical temperature is determined by  $\alpha'(1-t) = K_{1234}(\pi/W)^2$ . We call this the  $A_2$  phase.

If both  $q_x$  and  $q_y$  are non-zero, both  $\eta_{x,\vec{q}}$ ,  $\eta_{y,\vec{q}}$  are finite. We define this kind of solution as B phase. To simplify the calculations, we ignore crystal anisotropy for the moment, and set  $K_4 = 0$ . From Eq.(3), we find the smallest eigenvalue is  $K_1 q^2$  (for  $K_{23} > 0$ ). To have the normal component to the surfaces at  $x = 0$  and  $L$  to vanish,  $\eta_x$  must have the factor  $\sin(m\pi x/L)$ , where  $m$  is an integer. Because the boundary conditions  $\partial\eta_x/\partial y = 0$  at  $y = 0$  and  $W$ ,  $\eta_x$  should be proportional to  $\cos(n\pi y/W)$ , with  $n$  also an integer. We can use the same arguments for  $\eta_y$ . Therefore

$$\begin{aligned} \eta_x &= X \sin \frac{m\pi x}{L} \cos \frac{n\pi y}{W}, \\ \eta_y &= Y \cos \frac{m\pi x}{L} \sin \frac{n\pi y}{W}. \end{aligned} \quad (4)$$

The critical temperature is highest for  $m = n = 1$ , and thus determined by  $\alpha'(1-t) = K_1[(\pi/L)^2 + (\pi/W)^2]$ . In order to satisfy Eq.(3), we need  $(\pi/L)X + (\pi/W)Y = 0$ , which means  $X$  and  $Y$  are relatively real and have opposite signs.

Comparing the transition temperatures of the A and B phases, we find that the system prefers the  $A_1$  phase for  $L \gg W$ . For  $L \sim W$ , it prefers the B phase. We define

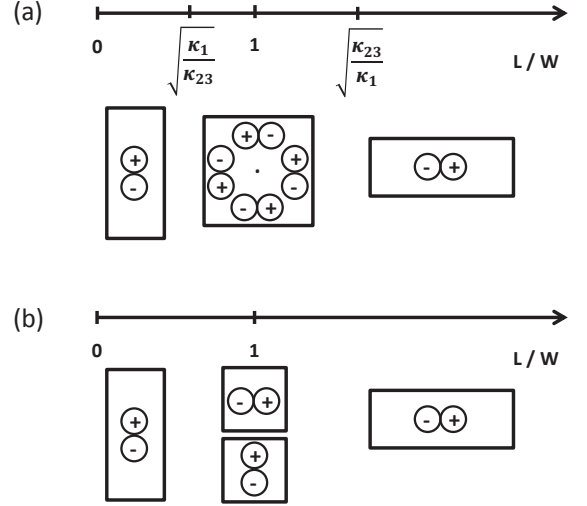


FIG. 1: GL phase diagram at the transition temperature.  $K_4 = 0$ . (a)  $K_{23}/K_1 > 1$  (b)  $K_{23}/K_1 < 1$ .

the aspect ratio of the sample as  $\rho = L/W$ . The critical aspect ratio separating these two phases is

$$\rho_c = \sqrt{K_{23}/K_1}. \quad (5)$$

With the same reasoning, the system is in  $A_2$  phase for  $W \gg L$  but prefers the B phase if  $\rho$  is larger than  $\rho_c^{-1} = \sqrt{K_1/K_{23}}$ . The phase diagram is shown in Fig.1(a). The cartoon pictures under the ruler are used to specify main characteristic of the order parameter in the corresponding phases. The solution for the middle case (B phase) is qualitatively same as the circular disk in [13]. Because the relatively real coefficients in Eq.(4), we can represent  $\vec{\eta}$  by a real vector, as done in the inset of Fig.2(c). It is clear that the order parameter forms a vortex-like structure, and vanishes at the sample center.

When crystal anisotropy is included, the critical ratio becomes

$$\rho_c = \sqrt{\frac{K_{1234}K_{234} - K_4(K_{23} + K_{234})}{K_1 K_{1234}}}. \quad (6)$$

It reduces to Eq.(5) for  $K_4 = 0$ . For small  $K_4$ , the critical ratio is  $\sqrt{2 - K_4/K_{123}}$  within the weak-coupling limit. It shows that the crystal anisotropy for  $K_4 > (<)0$  stabilizes(destabilizes) the order parameter with the direction parallel to the long side of the sample. The phase diagram is similar to Fig.1(a) except smaller(larger) region for vortex state. We ignore crystal isotropy in the following.

With decreasing  $K_{23}/K_1$ , the stability region for B phase becomes narrower. This phase diagram (Fig.1(a)) will change qualitatively if  $K_1 > K_{23}$ . The B phase is never stable (at  $T_c$ ), and the system is in the  $A_1$  phase if  $\rho > 1$ , and in the  $A_2$  phase if  $\rho < 1$ . The square

sample  $\rho = 1$  forms a special case, where the system still has  $C_4$  symmetry in real space, and the  $A_1$  and  $A_2$  phases are therefore degenerate. One can combine these two solutions with a phase difference. As a result, if the higher order terms in eq (1) for the bulk free energy prefer a time-reversal-symmetry-broken state, then the system would enter such a state directly at  $T_c$ . Therefore, the phase diagram becomes Fig.1(b) for  $K_{23} < K_1$ , where the ground state at  $\rho = 1$  should break the time-reversal symmetry. [18]

Our results for the square here provide further understanding of those we obtained earlier for the circular disk [13]. There, we found that, for  $K_{1,2,3}$  near the weak-coupling values ( $K_1 = K_2 = K_3$ ) the phase transition from the normal state is always to the state (named  $n = 1$  there) which preserves time-reversal but with a vortex at the center. That phase obviously has the same qualitative behavior as our B phase here. For sufficiently small  $K_{23}/K_1$ , we found that the system can enter a broken time-reversal symmetry state directly. We find the same results here though the critical value for  $K_{23}/K_1$  obviously can depend on the geometry.

In order to check the validity of the phase diagram from GL theory, we employ quasi-classical (QC) Green's function theory. For simplification, we focus on the isotropic and weak-coupling case. As shown in Ref.[13], we have, after linearizing in the order parameter,

$$(2i\epsilon_n + iv_f \hat{p} \cdot \vec{\nabla})f = 2i\pi(\text{sgn}\epsilon_n)\Delta, \quad (7)$$

where  $f(\hat{p}, \epsilon_n, \vec{r})$  and  $\Delta(\hat{p}, \vec{r})$  describe separately the off-diagonal parts of the QC propagator and pairing function,  $\hat{p}$  is the momentum direction,  $\epsilon_n$  is Matsubara frequency, and  $v_f$  is the Fermi velocity. With pairing interaction written as  $V_1 \hat{p} \cdot \hat{p}'$ , the gap equation reads

$$\Delta(\hat{p}, \vec{r}) = N(0)TV_1 \sum_n \langle (\hat{p} \cdot \hat{p}')f(\hat{p}', \vec{r}, \epsilon_n) \rangle \quad (8)$$

where the angular bracket denotes angular average over  $\hat{p}'$  and  $N(0)$  is the density of states at the Fermi level. For our square geometry and assuming smooth surfaces, we have the boundary conditions  $f(\theta) = f(\pi - \theta)$  at  $x=0$  and  $L$  and  $f(\theta) = f(-\theta)$  at  $y=0$  and  $W$ . Here  $\theta$  is the angle between  $\hat{p}$  and  $\hat{x}$ .

Before solving the case in a confined rectangle, we like to mention the connection between GL theory and QC theory for the bulk. To zeroth order in gradient, one finds

$$1 = \pi N(0)V_1 T_c^0 \sum_{\epsilon_n} \frac{1}{2|\epsilon_n|}, \quad (9)$$

which defines the bulk transition temperature  $T_c^0$ . The first order for  $f$  is odd in  $\epsilon_n$  and will not contribute to the gap equation. In the second order, we recover the GL theory with

$$\frac{K_1}{\alpha'} = 2\pi T_c^0 \sum_{\epsilon_n} \frac{v_f^2}{4|\epsilon_n|^3} \langle \cos^2 \theta \sin^2 \theta \rangle, \quad (10)$$

and similar expressions for  $K_{2,3}$ , with  $K_1 = K_2 = K_3$ . Our equations are consistent with those in Ref. [1, 2, 16]

For the  $A_1$  phase, we shall show that we can have a self-consistent solution in QC theory with

$$\Delta(\hat{p}, \vec{r}) = X \sin \frac{\pi x}{L} \cos \theta, \quad (11)$$

the order parameter suggested by the GL theory. One finds that  $f$  is independent of  $y$ . With the ansatz

$$f(\theta, \epsilon_n; x) = C_1(\theta, \epsilon_n) \sin \frac{\pi x}{L} + C_2(\theta, \epsilon_n) \cos \frac{\pi x}{L} \quad (12)$$

satisfying the boundary conditions, solving for  $C_{1,2}(\theta, \epsilon_n)$  via eq.(7) and using (9), we find

$$\ln \frac{T_c^0}{T_c} = 2\pi T_c \sum_{\epsilon_n=-\infty}^{\infty} \left\langle \frac{(\frac{v_f \pi}{L})^2 \cos^4 \theta}{4|\epsilon_n|^3 [1 + \frac{(\frac{v_f \pi}{L} \cos \theta)^2}{4\epsilon_n^2}]} \right\rangle. \quad (13)$$

For large  $L$ , one can replace the bracket in the denominator by 1, the LHS by  $(1 - t)$ , recovering the GL result using Eq.(10). Hence we see that, beyond GL, one needs simply to include extra factors in the denominator of Eq.(13) and include the  $\ln$  on the LHS.

Now, we consider the B phase. The order parameter is

$$\Delta(\hat{p}, \vec{r}) = X \sin \frac{\pi x}{L} \cos \frac{\pi y}{W} \cos \theta + Y \cos \frac{\pi x}{L} \sin \frac{\pi y}{W} \sin \theta. \quad (14)$$

From previous experience, it suggests that the solution has the following form

$$f = C_1(\theta, \epsilon_n) \sin \frac{\pi x}{L} \cos \frac{\pi y}{W} + C_2(\theta, \epsilon_n) \cos \frac{\pi x}{L} \sin \frac{\pi y}{W} + C_3(\theta, \epsilon_n) \cos \frac{\pi x}{L} \cos \frac{\pi y}{W} + C_4(\theta, \epsilon_n) \sin \frac{\pi x}{L} \sin \frac{\pi y}{W}. \quad (15)$$

To simplify writing, let  $A = \pi v_f/L$ ,  $B = \pi v_f/W$ . Again solving for  $f$  from (7), we obtain the following coupled linear equations in  $X, Y$ :

$$X \ln \frac{T_c^0}{T_c} = 2\pi T_c \sum_{\epsilon_n} \left\langle \frac{[(c_1 + c_2) \cos^2 \theta]X + c_3 Y}{|\epsilon_n|D} \right\rangle. \quad (16)$$

$$Y \ln \frac{T_c^0}{T_c} = 2\pi T_c \sum_{\epsilon_n} \left\langle \frac{[(c_1 + c_2) \sin^2 \theta]Y + c_3 X}{|\epsilon_n|D} \right\rangle. \quad (17)$$

Here  $c_1 = (A^2 \cos^2 \theta + B^2 \sin^2 \theta)/(4\epsilon_n^2)$ ,  $c_2 = (A^2 \cos^2 \theta - B^2 \sin^2 \theta)/(4\epsilon_n^2)$ ,  $c_3 = (AB \sin^2 \theta \cos^2 \theta)/(2\epsilon_n^2)$ , and  $D = 1 + 2c_1 + c_2$ . The critical temperature of the B phase is determined by the point which allows non-trivial  $X$  and  $Y$ . We note that if one keeps only the lowest orders in  $A^2$  and  $B^2$ ,  $D \rightarrow 1$ , and replaces the  $\ln$ 's on LHS by  $(1 - t)$ , then Eq.(16) and Eq.(17) recover the corresponding equations (3) in GL theory.

In Fig.2(a), we compare the critical temperatures for different sizes of square samples between GL and QC theories. We use the coherence length  $\xi \equiv \sqrt{K_{123}/\alpha'}$  as the unit for length ( $\xi = 0.199909 v_f/T_c^0$  for QC). In GL theory,  $(1 - t)$ , the relative suppression of critical temperature, is inversely proportional to the square of the

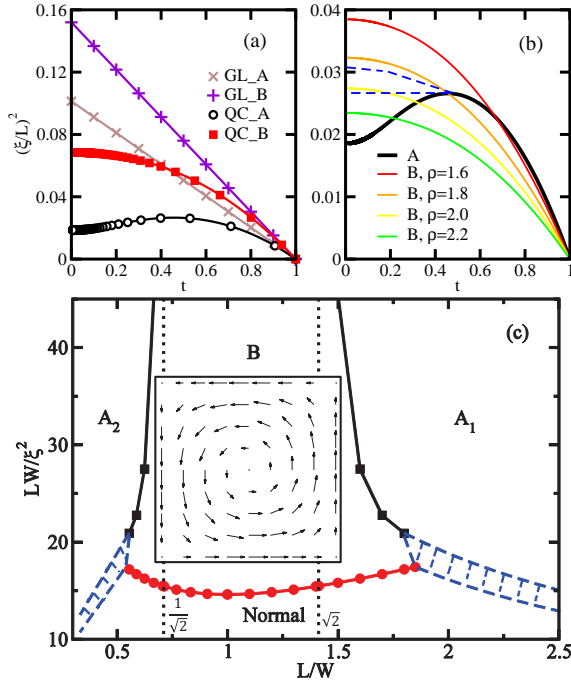


FIG. 2: (a) Critical temperatures from GL and QC theories for square samples. (b) Critical temperatures in QC theory for different  $\rho$ 's. As the size of the system is reduced, the ground state near the critical temperature can change from A to B. The possible first order phase transition is indicated in the region between dash lines. (c) Phase diagram for different sizes. Lines with squares or circles correspond to the second order phase transition; a first order transition line lies within each dashed region. Inset: Order parameter for a square sample. Note that all results are for  $K_1 = K_2 = K_3$ .  $\xi$  is the coherence length.

length scale of the system. Therefore it is more convenient to set the vertical axes of the phase diagram to be  $(\xi/L)^2$ . We obtain the straight line with crosses for the critical temperature of A phase and the line with pluses for that of B phase. It shows that the system prefers the B phase. On the other hand, we also present the critical temperatures calculated from QC theory. The line with squares is for the B phase and the line with circles is for the A phase. As expected, it shows that the results from QC theory are consistent with those from GL theory near  $t = 1$  which is corresponding to the bulk system ( $\xi/L \rightarrow 0$ ). In addition to the fact that the B phase is still preferred, we see that the critical temperature is more suppressed than GL as the size of the system is

smaller. [19]

As the aspect ratio  $\rho$  becomes larger than 1, GL theory shows that there is a phase transition from the B phase to the A phase as  $\rho$  increases beyond the critical ratio  $\sqrt{K_{23}/K_1}$  (Fig.1(a)). In Fig.2(b), we find that this critical ratio ( $\sqrt{2}$  here) still applies for large systems. However, we find that the B phase occupies a slightly larger  $\rho$  region when the size decreases. An example is in Fig.2(b), where we show that the system processes a phase transition from the A phase (thick black line) to the B phase for  $\rho = 1.6$  (thin red line) around  $t = 0.67$  as the size of the system becomes smaller. As the aspect ratio decreases further, the situation becomes more complicated because the phase boundary for A phase is not a monotonic function in  $t$ . From the shape of the curve, we expect that we have a first order phase transition at lower temperatures (cf. [20]). We shall leave the detailed investigation of this first order phase transition for the future. For illustrative purposes, we indicate the resulting phase diagram by postulating a first order transition line somewhere between the two dashed lines in Fig.2(b). Our obtained phase diagram is summarized in Fig.2(c). Here, instead of using  $(\xi/L)^2$  as the vertical axes, we use the area of the sample. Fig.2(c) shows that for very small sample within the QC limit, the system is normal and not superconducting. As the size of the system is larger, one can get the A phase via a first order phase transition for sufficiently large or small aspect ratios, or otherwise the B phase via a second order phase transition. The B phase with the aspect ratio larger than  $\sqrt{2}$  or smaller than  $1/\sqrt{2}$  can have another phase transition into A phase. For very large samples, we recover the critical ratios  $\sqrt{2}$  and  $1/\sqrt{2}$ , consistent with the results from GL theory. For the square samples, the stable phase is the B phase, with a vortex-like structure at the center, similar to the  $n = 1$  state in [13] obtained in the disk geometry.

In conclusion, we studied a two-component p-wave superconductor in a rectangular geometry near its transition temperature. The order parameter can behave differently depending on the aspect ratio and size. The phase always preserves time-reversal symmetry, except for a square with parameters rather far away from isotropic weak-coupling theories. Our results give further support to those obtained in [13] but not [21].

This work is supported by the National Science Council of Taiwan under grant number NSC 101-2112-M-001-021-MY3.

[1] A. J. Leggett, Rev. Mod. Phys. **47**, 331 (1975).  
 [2] D. Vollhardt and P. Wölfle, The Superfluid Phases of Helium 3, Taylor and Francis, London (1990).  
 [3] J. A. Sauls, Advances in Physics, **43**, 113 (1994).  
 [4] Robert Joynt and Louis Taillefer, Rev. Mod. Phys. **74**,

235 (2002).  
 [5] A. P. MacKenzie and Y. Maeno, Rev. Mod. Phys. **75**, 657 (2003).  
 [6] Y. Maeno, S. Kittaka, T. Nomura, S. Yonezawa, and K. Ishida, J. Phys. Soc. Jpn. **81**, 011009 (2012).

- [7] J. Jang *et al*, Science **331**, 186 (2011).
- [8] X. Cai, Y. A. Ying, N. E. Staley, Y. Xin, D. Fobes, T. Liu, Z. Q. Mao, and Y. Liu, arXiv:1202.3146.
- [9] M. Matsumoto and M. Sigrist, J. Phys. Soc. Jpn. **68**, 994 (1999); **68**, 3120 (E) (1999);
- [10] M. Stone and R. Roy, Phys. Rev. B **69**, 184511 (2004);
- [11] J. A. Sauls, Phys. Rev. B **84**, 214509 (2011)
- [12] M. Sigrist and H. Monien, J. Phys. Soc. Jpn. **70**, 2409 (2001). H. Kaneyasu, N. Hayashi, B. Gut, K. Makoshi, and M. Sigrist, J. Phys. Soc. Jpn. **79**, 104705 (2010).
- [13] Bor-Luen Huang and S.-K. Yip, Phys. Rev. B **86**, 064506 (2012).
- [14] Recently, V. Vakaryuk (Phys. Rev. B **84**, 214524 (2011)) has claimed that by considering the magnetic energy, a mesoscopic sample of  $\text{Sr}_2\text{RuO}_4$  could also favor a time-reversal symmetry state. His mechanism, however, is completely different from us.
- [15] Eq.(2) can also be rewritten as  $\{K'_1|\partial_x\eta_x|^2 + K'_2|\partial_y\eta_x|^2 + K'_3(\partial_x\eta_y)(\partial_y\eta_x)^* + K'_4(\partial_y\eta_x)(\partial_x\eta_y)^*\} + \{x \leftrightarrow y\}$ , the same form as in Ref.[16] with  $K'_1 = K_{1234}$ ,  $K'_2 = K_1$ ,  $K'_3 = K_2$ , and  $K'_4 = K_3$ .
- [16] D. F. Agterberg, Phys. Rev. Lett. **80**, 5184 (1998).
- [17] V. Ambegaokar, P. de Gennes and D. Rainer, Phys. Rev. A **9**, 2676 (1974); **12**, 345 (E) (1975).
- [18] On the other hand, if the higher order terms in eq (1) favor a time-reversal symmetric state for the bulk, then the system at  $\rho = 1$  would then be either in the  $A_1$  or  $A_2$  phase, thus spontaneously breaking the  $C_4$  rotational symmetry. We thus believe that the speculation in our footnote 27 in ref [13] is probably incorrect.
- [19] In our previous study [13] in circular disks, we found instead that the critical temperature is independent of the radius  $R$ . We speculate that the present suppression of  $T_c$  is due to the existence of corners.
- [20] G. Sarma, J. Phys. Chem. Solids, **24**, 1029 (1963).
- [21] J. W. Huo, W-Q. Chen, S. Raghu and F-C. Zhang, Phys. Rev. Lett. **108**, 257002 (2012)